



Since January 2020 Elsevier has created a COVID-19 resource centre with free information in English and Mandarin on the novel coronavirus COVID-19. The COVID-19 resource centre is hosted on Elsevier Connect, the company's public news and information website.

Elsevier hereby grants permission to make all its COVID-19-related research that is available on the COVID-19 resource centre - including this research content - immediately available in PubMed Central and other publicly funded repositories, such as the WHO COVID database with rights for unrestricted research re-use and analyses in any form or by any means with acknowledgement of the original source. These permissions are granted for free by Elsevier for as long as the COVID-19 resource centre remains active.



Development of highly stable and de-immunized versions of recombinant alpha interferon: Promising candidates for the treatment of chronic and emerging viral diseases

Sofía Inés Giorgetti^a, Marina Etcheverrigaray^a, Frances Terry^b, William Martin^b, Anne Searls De Groot^{b,c}, Natalia Ceaglio^a, Marcos Oggero^a, Eduardo Federico Mufarrege^{a,*}

^a UNL, CONICET, FBCB (School of Biochemistry and Biological Sciences), CBL (Biotechnological Center of Litoral), Ciudad Universitaria, Ruta Nacional 168 Km 472.4, C.C. 242. (S3000ZAA), Santa Fe, Argentina

^b EpiVax, Inc., Providence, RI, USA

^c Institute for Immunology and Informatics, University of Rhode Island, RI, USA

ARTICLE INFO

Keywords:

Alpha interferon
Antiviral therapy
T cell epitope
In silico prediction
De-immunization
COVID-19

ABSTRACT

Human interferon alpha (hIFN- α) administration constitutes the current FDA approved therapy for chronic Hepatitis B and C virus infections. Additionally, hIFN- α treatment efficacy was recently demonstrated in patients with COVID-19. Thus, hIFN- α constitutes a therapeutic alternative for those countries where vaccination is inaccessible and for people who did not respond effectively to vaccination. However, hIFN- α 2b exhibits a short plasma half-life resulting in the occurrence of severe side effects. To optimize the cytokine's pharmacokinetic profile, we developed a hyperglycosylated IFN, referred to as GMOP-IFN.

Given the significant number of reports showing neutralizing antibodies (NAb) formation after hIFN- α administration, here we applied the DeFT (De-immunization of Functional Therapeutics) approach to develop functional, de-immunized versions of GMOP-IFN. Two GMOP-IFN variants exhibited significantly reduced *ex vivo* immunogenicity and null antiproliferative activity, while preserving antiviral function. The results obtained in this work indicate that the new de-immunized GMOP-IFN variants constitute promising candidates for antiviral therapy.

1. Introduction

The emergence of new viral threats, such as the severe acute respiratory syndrome coronavirus 2 (SARS-CoV-2) reveals the necessity of effective therapeutic alternatives. This is particularly relevant for those countries where vaccination is not accessible. In addition, the use of hIFN- α can be a suitable therapeutic alternative for people in whom the vaccine against SARS-CoV-2 is less effective or not effective at all. Recently, a study involving 2165 positive COVID-19 patients treated with hIFN- α showed a significant reduction in the likelihood of intensive care as well as an improvement in the survival rate for patients suffering serious diseases [1]. In addition, hIFN α 2a, hIFN α 2b and their pegylated forms, in combination with ribavirin or favipiravir, have also been considered suitable strategies to treat patients with COVID-19 [2–6].

Dengue virus (DENV), Chikungunya virus (CHIKV) and Zika virus (ZIKV) infections also constitute a significant challenge for world-wide

public health.

Dengue is the most prevalent mosquito-borne viral illness in humans, caused by four genetically and serologically related viruses, which are transmitted by the mosquito vectors *Aedes aegypti* and, to a lesser extent, *Aedes albopictus*. DENV infection produces clinical manifestations characterized by hemorrhagic fever and shock syndrome [7,8].

The widely distributed *Aedes* mosquito is the main vector of ZIKV. However, transmission through secretions (saliva, urine), sexual contact, and perinatal contagion have also been reported. ZIKV infection is associated with severe neurologic manifestations, such as Guillain-Barré syndrome and congenital microcephaly in newborns and fetuses [9,10]. For this, ZIKV was declared as a “Public Health Threat of International Concern” (WHO, www.who.int).

CHIKV is an enveloped alphavirus also transmitted through an *Aedes* mosquito vector that causes high fever, polyarthralgias (joint pain), headache, myalgias, and polyarthritis, among others [11]. Although the

* Corresponding author at: Ciudad Universitaria, Ruta Nacional 168 - Km 472.4 - C.C. 242 - (S3000ZAA), Santa Fe, Argentina.

E-mail address: mufarrege@fbc.unl.edu.ar (E.F. Mufarrege).

<https://doi.org/10.1016/j.clim.2021.108888>

Received 17 August 2021; Received in revised form 4 October 2021; Accepted 13 November 2021

Available online 17 November 2021

1521-6616/© 2021 Elsevier Inc. All rights reserved.

acute phase persists by almost a week, arthralgias may last for months or even years, negatively affecting the patient's life quality and their ability to continue daily activities, contributing to the economy of endemic areas [12].

So far, there are no commercially available prophylactic or therapeutic drugs effective against human DENV, CHIKV nor ZIKV infections, thus limiting treatment of the infections to supportive therapies like corticosteroids, antipyretics or nonsteroidal anti-inflammatory drugs, all of which have numerous side effects associated to excessive self-medication [13,14]. Considering the rapid dissemination of these viruses to new regions and consequently the increasing number of human infections, the identification of new antiviral candidates or the use of effective pre-existing therapies against them has become a public health priority.

As anti-viral therapy, the use of recombinant human alpha interferon (rhIFN- α) combined with favipiravir has provided substantial ZIKV inhibition *in vitro*, leading to complete virus suppression without exhibiting cytotoxicity to uninfected host cells even when elevated doses were tested [13]. Moreover, an *in vitro* study using Huh7 cells treated with Sofosbuvir plus rhIFN- α revealed a significant decrease in the number of remaining infected cells (4.3–7.3%) compared to treatment with either rhIFN- α alone (8.2–17.2%) or sofosbuvir alone (30–46%), revealing the synergistic effect against different human ZIKV strains when both drugs are used in combination [11]. Additionally, rhIFN- α alone or in combination with ribavirin has also shown to be selective and efficacious against DENV and CHIKV replication *in vitro*, showing the highest potency among a panel of different antiviral compounds tested [15,16]. More recently Schitle et al. have also demonstrated the highly synergistic activity of ribavirin and rhIFN- α as combined therapy, reducing CHIKV burden by at least 99% during the first 24 h of treatment [17]. These findings strongly support the use of rhIFN- α as a promising treatment for these emerging viral pathologies.

hIFN- α s comprise a multigene family of cytokines that participate in antiviral mechanisms, immune modulation and cell growth regulation. hIFN- α s are normally expressed at very low levels in leukocytes in response to a number of stimuli such as virus infections, foreign antigens, cytokines and growth factors [18]. Their production is mainly triggered by Toll like receptors (TLR) signaling and their action is mediated through JAK/STAT (Janus kinase/Signal Transducers and Activators of Transcription) and other signaling pathways [19].

Two recombinant allelic versions of hIFN- α (rhIFN- α 2a and rhIFN- α 2b) have shown remarkable therapeutic properties for the treatment of numerous viral diseases such as AIDS related Kaposi's sarcoma and chronic hepatitis B and C, among others [20,21].

A major disadvantage of rhIFN- α 2b therapy is its short plasma half-life –due to rapid renal clearance, strong binding to specific receptors and proteolytic degradation in blood– which results in frequent and high dose administrations, leading to the development of severe side effects [18]. In order to optimize the cytokine's pharmacokinetic profile, two forms of rhIFN- α 2 conjugated with polyethylene glycol have been successfully developed (PEGINTRON®, by Schering Plough, and PEGASYS®, by Roche), improving its efficacy when compared with the native molecule. However, it has been reported that failure of treatment with pegylated rhIFN- α in chronic hepatitis C patients may be due to the development of neutralizing anti-rhIFN- α antibodies [22–24]. In line with this notion, *ex vivo* studies carried out by our group revealed that a number of T cells clones from different HLA-DRB1 donor samples were activated upon incubation with the pegylated version of the cytokine [25].

In an attempt to improve the *in vivo* rhIFN- α bioavailability we developed new rhIFN- α 2b variants by introducing four potential N-glycosylation consensus sequences [26]. This strategy led to the development of a hyperglycosylated protein, 4 N-IFN, with a 25-fold longer plasma half-life than the unmodified molecule. However, subsequent *in silico* and *ex vivo* studies revealed that the modifications may have increased the immunogenic potential of this recombinant protein. For

this reason, we performed a step-wise approach to reduce 4N-IFN immunogenicity. New, de-immunized variants of 4 N-IFN exhibited reduced *ex vivo* immunogenicity but also a significant reduction in their antiviral activity [25].

To circumvent this issue, we then developed a highly O-glycosylated rhIFN- α 2b by fusing the N-terminal end of the cytokine to a peptide derived from human granulocyte and macrophage-colony stimulating factor that contains four potential O-glycosylation sites, designated as GMOP (GM-CSF O-glycosylated Peptide). This strategy avoided an extensive protein structure modification, and the new variant (GMOP-IFN) retained full *in vitro* specific activity of the unmodified rhIFN- α 2b (WT-IFN) produced in CHO-K1 cells and remarkably improved pharmacokinetic parameters [27].

To further characterize this protein, in this study we performed an *in silico* immunogenicity analysis, which revealed that GMOP-IFN is potentially immunogenic. To decrease or even suppress the number of T-cell epitopes in the protein sequence, we followed a stepwise de-immunization procedure. This strategy is called *Deimmunization for Functional Therapeutics* or “DeFT” which can identify T cell epitopes inside the protein and then suggests suitable modifications to reduce their ability to bind to prevalent MHCII molecules, while preserving protein function [28].

The *in silico* analysis using EpiMatrix and ClustiMer revealed a high content of T cell epitopes into the GMOP-IFN sequence [29]. Then, by using the OptiMatrix program we introduced specific mutations in order to disrupt the MHC interaction with multiple HLA alleles. Ten modifications were selected as candidates to be introduced in different combinations to generate four de-immunized GMOP-IFN variants, which were designated as GMOP-IFN-(VAR1–4).

2. Methods

2.1. Deimmunization tools

To deimmunize GMOP-IFN, an *in silico* analysis previously described by Moise et al. [28], was carried out. The sequence of GMOP-IFN was partitioned into overlapping 9-mer frames and then each frame was assessed against eight archetypal HLA class II alleles in terms of its immunogenic potential. The HLA class II alleles included in the study represent [at least, or over] 90% of MHC diversity in the human population, namely DRB1*0101, DRB1*0301, DRB1*0401, DRB1*0701, DRB1*0801, DRB1*1101, DRB1*1301 and DRB1*1501 [32]. For all 9-mer fragments a “Z” score was assigned by EpiMatrix, as a measurement of the chance of binding to the MHCII molecule. Every 9-mer peptide scoring above 1.64 on the EpiMatrix “Z” scale is appointed as a “hit” and correspond to the top 5% of the peptide set with a significant chance of MHCII binding. 9-mers peptides scoring above 2.32 (which correspond to the top 1%) have extremely high probabilities to bind. Most published T cell epitopes fit into this category. With these results and using the ClustiMer tool, the number of concentrated regions with high potential of binding to different MHC molecules was assessed. Regions scoring above 10 (which includes multiple ‘hits’ against a diversity of HLA DR alleles) were identified as those of high immunogenicity potential [33]. Finally, by using OptiMatrix, an additional EpiVax ISPRI toolkit for deimmunization, the individual contribution of each amino acid to MHCII molecules binding was analyzed. This program identifies key residues for MHC binding across every 9-mer frames and HLA alleles. Then OptiMatrix iteratively replaces the alternative 19 amino acids in a specific position of a peptide sequence and re-predicts immunogenicity for the new sequence. To prevent the negative impact of each mutation on protein structure and biological function, data from several published studies were taken into account when establishing the residues not suitable for being modified in IFN-alpha in order to reduce its immunogenicity (please see table 1 in Mufarrege et al. 2017) [25].

2.2. Gene expression in mammalian cells

2.2.1. Cell culture

Human Embryonic Kidney (HEK293T/17 ATCC® CRL-11268) were grown in Dulbecco's modified Eagle Medium (DMEM, Gibco, USA) with 10% (v/v) fetal calf serum (FCS, PAA, Argentina) and 2 mM glutamine.

Chinese Hamster Ovary (CHO-K1, ATCC® CCL-61) cells were cultured in DMEM/Ham's F12 medium (Gibco, USA), supplemented either with 5% (v/v) FCS (growth medium) or 0,5% (v/v) FCS (production medium).

Madine Darby Bovine Kidney (MDBK, ATCC® CCL-22) cells were grown in minimum essential medium (MEM; Gibco, USA) supplemented with 10% (v/v) FCS (growth medium). Antiviral activity assays were performed using MEM medium supplemented with 2% (v/v) FCS (assay medium).

Human Daudi cell line was obtained from the Deutsche Sammlung von Mikroorganismen und Zellkulturen GmbH (DSMZ; Braunschweig, Germany) culture collection (DSMZ n°: ACC 78). Daudi cells and human Peripheral Blood Mononuclear Cells (PBMCs) were cultured in Roswell Park Memorial Institute 1640 medium (RPMI, Gibco, USA) with 10% (v/v) FCS. The same medium was then used for bioassays.

All cell cultures were maintained at 37 °C in humidified 5% CO₂.

2.2.2. Construction of lentiviral vectors and assembly of lentiviral particles

Plasmids carrying the hIFN- α 2b encoding sequence (GeneWiz, USA) were digested with *SalI* and *XbaI* enzymes and the released DNA fragments corresponding to each GMOP-IFN variant were cloned into a lentiviral plasmid (pLV). All construct identities were verified by DNA sequencing.

Research grade HIV-based LV particles containing the four hIFN- α 2b analog transgenes were produced following the protocol suggested by Naldini et al. [34] and Dull et al. [35]. Adherent HEK293T cells were cultured in 10 cm-plates and simultaneously co-transfected with four plasmids: the packaging plasmid (pMDLg/pRRE) [35], the Rev-expressing plasmid (pRSV-Rev) [34], the envelop plasmid expressing VSV-G (pMD2.G) [35], and the corresponding transfer vectors containing the transgenes (pLVs). Plasmid internalization into cells was achieved by liposome-mediated gene transfer, using LipofectAMINE 2000 Reagent (Invitrogen, USA), following the supplier's instructions. Supernatants containing lentiviral particles (LVPs) were harvested 72 h post-transfection.

2.2.3. Lentiviral transduction

Transductions were carried out by incubating 6.0×10^4 cells per well seeded onto 6-well plates (Greiner, Germany) with 1 ml of supernatants containing LVPs. 24 h post-transduction culture medium was changed to fresh medium. In order to eliminate the remaining wild type cells, 96 h post-transduction a selective pressure process was started by replacing supernatants with fresh growth medium containing $10 \mu\text{g}\cdot\text{ml}^{-1}$ puromycin (Sigma Aldrich, USA). Selective medium was changed every 3–4 days with increasing puromycin concentrations until control cell death.

2.2.4. GMOP-IFN variants production and purification

For GMOP-IFN variants production, transduced CHO K1 cells were amplified and each cell line's productivity was analyzed by quantification of rhIFN- α 2b and cell count determination. Cells were cultured in growth medium until reaching confluence using 500 cm² triple flasks (Thermo, USA) and then the medium was changed to production medium. Every 48 or 72 h, conditioned medium was harvested, centrifugated for its clarification and stored at -20 °C, while fresh production medium was added to producing cells. All GMOP-IFN variants were purified by immunoaffinity chromatography using the mAb CA5E6, an anti-non-glycosylated rhIFN- α 2b monoclonal antibody obtained and characterized in the Biotechnological Center of Litoral of the School of Biochemistry and Biological Sciences (Universidad Nacional del Litoral, Santa Fe, Argentina) [26]. This mAb coupled to CNBr-

activated Sepharose 4B (GE Healthcare, USA) has proved to bind effectively different IFN mutants [26]. All purified proteins were diluted in excipient. By excipient, we mean phosphate buffered saline (PBS), which is an inactive substance that serves as the vehicle for interferon alpha in this study. The concentration of purified GMOP-IFN variants was determined by spectrophotometric quantification ($\lambda = 280$) considering the corresponding molar extinction coefficient (EC) for each protein variant (Table 1, Supplementary Material).

2.3. Physicochemical characterization

2.3.1. rhIFN- α sandwich ELISA

GMOP-IFN variants in culture supernatants were quantified by sandwich ELISA assay as it was previously described by Ceaglio and collaborators [26]. GMOP-IFN variants in culture supernatants were quantified by sandwich ELISA assay as it was previously described by Ceaglio and collaborators. Briefly, 96-well plates were coated overnight at 4 °C with 100 ng per well of the monoclonal antibody CA5E6 in 50 mM carbonate-bicarbonate buffer (pH 9.6). After blocking 1 h at 37 °C with 1% (w/v) BSA in phosphate-buffered saline (PBS), plates were incubated with 1:2 serial dilutions of *E. coli* derived rhIFN- α 2b standard (Protech Pharma, Argentina) from 10 ng ml^{-1} to 0.16 ng ml^{-1} or 1:2 serial dilutions of GMOP-IFN variants for 1 h at 37 °C. Subsequently, plates were treated with a dilution of rabbit anti-rhIFN- α 2b pAb for 1 h at 37 °C. Finally, peroxidase-labeled goat anti-rabbit immunoglobulins (DAKO, Denmark) diluted 1:1000 were added to the wells. After 1 h incubation, plates were incubated with substrate solution (0.5 mg ml^{-1} o-phenylenediamine, 0.015% (v/v) H₂O₂ in 50 mM phosphate-citrate buffer). Reaction was stopped by the addition of 2N H₂SO₄ and the absorbance was measured at 492 nm with a microtiter plate reader (Labsystems Multiskan MCC/340, Finland). Between every step, plates were washed with PBS containing 0.05% (v/v) Tween 20 (PBS-T). Dilutions were prepared in PBS-T containing 0.1% (w/v) BSA. The assay was reproduced in triplicate.

2.3.2. SDS PAGE and western blotting

Electrophoretic profiles were analyzed using SDS-PAGE with 5% (w/v) stacking gels and 15% (w/v) polyacrylamide resolving gels. Proteins were diluted in buffer containing 5% (v/v) beta-mercaptoethanol (J.T. Baker, USA) and electrophoretic separation was carried out at 200 V for 75 min. Gel staining was performed with Coomassie blue and destaining was achieved by incubation with a solution containing 15% (v/v) methanol and 10% (v/v) acetic acid. Non-glycosylated *E. coli*-derived hIFN- α 2b (GemaBiotech, Argentina) was used as control.

For western blot assays, transference of proteins onto the PVDF (polyvinylidene difluoride) membrane (BioRad, USA) was carried out. Then the membrane was blocked with 5% (w/v) non-fat milk in Tris-buffered saline (TBS) for 1 h and incubated with appropriately diluted rabbit anti-rhIFN- α 2b polyclonal antibodies for 1 h. Final incubation with the peroxidase-labeled goat anti-rabbit immunoglobulins (DAKO, Denmark) allowed visualization of reactive bands, using an ECL™ Chemiluminescent Western Blotting Analysis System (GE Healthcare, USA). Between every step, washes were performed using TBS with 0.05% (v/v) Tween 20. Dilutions were prepared in TBS containing 0.05% (v/v) Tween 20 and 0.5% (w/v) nonfat milk.

2.3.3. Isoelectric focusing (IEF)

To identify the different isoforms of GMOP-IFN and its de-immunized variants, a 1 mm thick 8% (w/v) polyacrylamide gel with 7 M urea was prepared. To establish the pH range, a mix of 30% (w/v) 5–7 ampholytes and 70% (w/v) 2–4 ampholytes (Pharmalyte, GE Healthcare, USA) was used. The gel was prefocused at 2000 V, 10 W and 100 mA for 30 min. Then, 5–20 μl samples were applied over a strip located at 1 cm from cathode and electrophoresis was performed under the conditions previously described for the prefocusing step for 90 min. Finally, separated components were visualized by Coomassie blue staining.

Table 1
Aminoacidic sequence of GMOP-IFN de-immunized variants.

GMOP-IFN-VAR1	1	2	3	4	5	6	7	8	9	10	11	12	13	14	15	16	17	18	19	20	21	22	23	24	25	26	27	28	29	30
	A P A S R P S P S L Q P W E C D L P Q T H S A G S R R T L M																													
	31	32	33	34	35	36	37	38	39	40	41	42	43	44	45	46	47	48	49	50	51	52	53	54	55	56	57	58	59	60
	A L A Q M R R I S L F S C L K D R H D F G G P Q E E F G N Q																													
	61	62	63	64	65	66	67	68	69	70	71	72	73	74	75	76	77	78	79	80	81	82	83	84	85	86	87	88	89	90
	A Q K A E T I P V L H E M I Q Q I F A A F S T K D S S A A W																													
	91	92	93	94	95	96	97	98	99	100	101	102	103	104	105	106	107	108	109	110	111	112	113	114	115	116	117	118	119	120
D E T L L D K F Y T E L Y Q Q L N D L E A C V I Q G V G V T																														
121	122	123	124	125	126	127	128	129	130	131	132	133	134	135	136	137	138	139	140	141	142	143	144	145	146	147	148	149	150	
E T P L M K E D S I A A V R K Y A Q R I T A Y L K E K K Y S																														
151	152	153	154	155	156	157	158	159	160	161	162	163	164	165	166	167	168	169	170	171	172	173	174	175	176	177	178	179		
P C A W E V V R A E T M R S F S L S T N A Q E S L R S K E																														
GMOP-IFN-VAR2	1	2	3	4	5	6	7	8	9	10	11	12	13	14	15	16	17	18	19	20	21	22	23	24	25	26	27	28	29	30
	A P A S R P S P S L Q P W E C D L P Q T H S A G S R R T L M																													
	31	32	33	34	35	36	37	38	39	40	41	42	43	44	45	46	47	48	49	50	51	52	53	54	55	56	57	58	59	60
	L L A Q M R R I S L F S C L K D R H D F G G P Q E E F G N Q																													
	61	62	63	64	65	66	67	68	69	70	71	72	73	74	75	76	77	78	79	80	81	82	83	84	85	86	87	88	89	90
	A Q K A E T I P V L H E M I Q Q I F N L F S T K D S S A A W																													
	91	92	93	94	95	96	97	98	99	100	101	102	103	104	105	106	107	108	109	110	111	112	113	114	115	116	117	118	119	120
D E T L L D K F Y T E L Y Q Q L N D L E A C V I Q G V G V T																														
121	122	123	124	125	126	127	128	129	130	131	132	133	134	135	136	137	138	139	140	141	142	143	144	145	146	147	148	149	150	
E T P L M K E D S I A A V R K Y A Q R I T A Y L K E K K Y S																														
151	152	153	154	155	156	157	158	159	160	161	162	163	164	165	166	167	168	169	170	171	172	173	174	175	176	177	178	179		
P C A W E V V R A E I M R S F S L S T N L Q E S L R S K E																														
GMOP-IFN-VAR3	1	2	3	4	5	6	7	8	9	10	11	12	13	14	15	16	17	18	19	20	21	22	23	24	25	26	27	28	29	30
	A P A S R P S P S L Q P W E C D L P Q T H S A G S R R T L M																													
	31	32	33	34	35	36	37	38	39	40	41	42	43	44	45	46	47	48	49	50	51	52	53	54	55	56	57	58	59	60
	L L A Q M R R I S L F S C L K D R H D F G G P Q E E F G N Q																													
	61	62	63	64	65	66	67	68	69	70	71	72	73	74	75	76	77	78	79	80	81	82	83	84	85	86	87	88	89	90
	A Q K A E T I P V L H E M I Q Q I F N L F S T K D S S A A W																													
	91	92	93	94	95	96	97	98	99	100	101	102	103	104	105	106	107	108	109	110	111	112	113	114	115	116	117	118	119	120
D E T L L D K F Y T E L Y Q Q L N D L E A C V I Q G V G V T																														
121	122	123	124	125	126	127	128	129	130	131	132	133	134	135	136	137	138	139	140	141	142	143	144	145	146	147	148	149	150	
E T P L M K E D S I A A V R K Y A Q R I T A Y L K E K K Y S																														
151	152	153	154	155	156	157	158	159	160	161	162	163	164	165	166	167	168	169	170	171	172	173	174	175	176	177	178	179		
P C A W E V V R A E T M R S F S L S T N A Q E S L R S K E																														
GMOP-IFN-VAR4	1	2	3	4	5	6	7	8	9	10	11	12	13	14	15	16	17	18	19	20	21	22	23	24	25	26	27	28	29	30
	A P A S R P S P S L Q P W E C D L P Q T H S A G S R R T L M																													
	31	32	33	34	35	36	37	38	39	40	41	42	43	44	45	46	47	48	49	50	51	52	53	54	55	56	57	58	59	60
	L L A Q M R R I S L F S C L K D R H D F G G P Q E E F G N Q																													
	61	62	63	64	65	66	67	68	69	70	71	72	73	74	75	76	77	78	79	80	81	82	83	84	85	86	87	88	89	90
	A Q K A E T I P V L H E M I Q Q I F A A F S T K D S S A A W																													
	91	92	93	94	95	96	97	98	99	100	101	102	103	104	105	106	107	108	109	110	111	112	113	114	115	116	117	118	119	120
D E T L L D K F Y T E L Y Q Q L N D L E A C V I Q G V G V T																														
121	122	123	124	125	126	127	128	129	130	131	132	133	134	135	136	137	138	139	140	141	142	143	144	145	146	147	148	149	150	
E T P L M K E D S I A A V R K Y A Q R I T A Y L K E K K Y S																														
151	152	153	154	155	156	157	158	159	160	161	162	163	164	165	166	167	168	169	170	171	172	173	174	175	176	177	178	179		
P C A W E V V R A E I M R S F S L S T N L Q E S L R S K E																														

Substitutions introduced in each sequence are depicted in red.

2.3.4. *In silico* prediction of O-glycosylation in GMOP-IFN variants

Given the lack of known consensus recognition sequences for the O-glycosyltransferases, neural network predictions of mucin type GalNAc O-glycosylation sites were performed by using the NetOGlyc 3.1 Server software [36].

2.4. *In vitro* activity assays

2.4.1. Antiviral assay

The ability of rhIFN- α 2b to inhibit the cytopathic effect caused by vesicular stomatitis virus (VSV, Indiana strain) on MDBK cells is a well

established method employed to determine the biological antiviral activity of the cytokine [37,38]. In order to evaluate the impact of modifications on the antiviral activity of de-immunized GMOP-IFN variants, MDBK cells were seeded into culture microtiter plates in growth medium (2.5×10^4 cells per well) and incubated at 37 °C overnight. Culture supernatants were removed and replaced by 1:2 serial dilutions of rhIFN- α 2b international standard (NIBSC 95/566), ranging from 20 IU·ml⁻¹ to 0.16 IU·ml⁻¹ or 1:2 serial dilutions of GMOP-IFN variants (test samples) in assay medium. Then, the plates were incubated for 6 h at 37 °C and, after removing the supernatants, the monolayers were infected with 1.6 PFU of VSV virus per cell. Viral replication was allowed to proceed until cell lysis was clearly observable in control wells (no rhIFN- α 2b). After virus incubation step, the supernatants were discarded and cells were fixed to the plate and stained with a solution of 0.75% (w/v) crystal violet in 40% (v/v) methanol during 15 min. After washing the plates with water, solubilization of remaining dye was achieved using a solution of 20% (v/v) acetic acid. Detection was made by reading the plates at 540 nm, utilizing a microtiter plate reader (Labsystems Multiskan MCC/340, Finland). The signal intensity of each sample dilution was calculated as the mean of the absorbance measured in five wells.

Finally, residual specific antiviral activities were calculated as the ratio of volumetric antiviral activity to protein concentration, determined by spectrophotometry.

2.4.2. Antiproliferative assay

In order to measure rhIFN- α 2b ability to inhibit cell growth, an *in vitro* bioassay using Daudi cells was carried out [39]. Serial 1:2 dilutions of rhIFN- α 2b WHO international standard (NIBSC 95/566) from 50 IU·ml⁻¹ to 0.02 IU·ml⁻¹ or GMOP-IFN variants test samples were placed into microtiter plate wells. Then, previously washed Daudi cells were added (5×10^3 cells per well) and plates were incubated at 37 °C for 96 h. Cell proliferation was determined using a CellTiter 96™ Aqueous Non-Radioactive Cell Proliferation Assay (Promega). Absorbance was read at 492 nm using a microplate reader. The assay was reproduced in triplicates.

2.5. Human PBMC preparation and HLA-DR typing

Blood samples from healthy donors aged between 18 and 60 years were obtained, after obtaining informed consent, by venipuncture. Blood extraction and handling procedures were previously approved by the Research Ethics Committee of the National University of Litoral, code number: CE2018-36 (Santa Fe, Argentina).

For PBMCs isolation, Ficoll-Paque™ PLUS (GE Healthcare Bio-Science, Switzerland) density gradient separation was performed according to manufacturer's instructions. Collected buffy coat was washed twice with PBS and PBMCs were cryopreserved in liquid nitrogen at a density of $1-3 \times 10^7$ cells·ml⁻¹. Previously an aliquot of blood was separated and HLA-DR allotypes were determined by Luminex Sequencing Technology (PRICAI, Buenos Aires, Argentina). Typing results were compared to publicly available HLA-DR frequencies in the world population: (www.allelefreqencies.net).

2.6. Immunogenicity assessment

2.6.1. Ex vivo T-cell assays

For *ex vivo* T-cell assays a modified protocol of a strategy previously described was performed [40]. Isolation of monocytes from each PBMC sample was achieved by differential adherence to culture plates [41]. The adherent cells were retained for differentiation and the non-adherent cells were collected and cryopreserved for further use. To induce the development of immature monocyte-derived dendritic cells (DC), monocytes were incubated in medium containing 1000 IU·ml⁻¹ of human IL-4 (Milipore, USA) and 1000 IU·ml⁻¹ of human GM-CSF (GemaBiotech, Argentina) during a period of 6 days, with a change of media at day 3. Immature DCs were collected on day 6, counted and

incubated with either GMOP-IFN variant (which means the original protein or one of its de-immunized variants) or non-antigen (PBS). After overnight incubation, DCs were washed to remove exogenous antigen, and resuspended in growth medium containing recombinant human tumor necrosis factor (rhTNF, ProsPec, USA) alpha, GM-CSF and IL-4 for 4 days, to induce DC maturation. Antigen pulsed-DCs were then incubated with autologous T cells for 48 h in medium containing 2 ng·ml⁻¹ human IL-2 (Thermo, USA). Supernatants were collected and evaluated for human IFN- γ and IL-4 quantification by sandwich ELISA. Negative control (PBS), and positive control with phytohemagglutinin (PHA, Sigma Aldrich, USA) were also included.

2.6.2. IFN- γ sandwich ELISA

96-well plates were coated with 100 μ l primary hIFN- γ mAb (clone NIB42, BD, USA) at a concentration of 2 μ g·ml⁻¹, first for 1 h at 37 °C and then overnight at 4 °C. After blocking 1 h at 37 °C with 1% (w/v) bovine serum albumin (BSA) in phosphate-buffered saline (PBS), culture supernatants were added and incubated for 2 h at 37 °C. Serial 1:2 dilutions of rhIFN- γ (BD, USA) from 1 ng·ml⁻¹ were also included. Then, 100 μ l/well of biotinylated hIFN- γ mAb (clone 4S-B3, BD, USA) at a concentration of 500 ng·ml⁻¹ was added to the plates and incubated for 1 h at 37 °C. Plates were subsequently incubated with streptavidin horseradish peroxidase conjugate (RPN4401-AMDEX, USA) diluted 1:5000. After 1 h, plates were incubated with substrate solution (0.5 mg·ml⁻¹ o-phenylenediamine, 0.015% (v/v) H₂O₂ in 50 mM phosphate citrate buffer). Reactions were stopped by the addition of 2N H₂SO₄ and the absorbance was measured at 492 nm with a microtiter plate reader (Labsystems Multiskan MCC/340, Finland). Between every step, plates were washed with PBS containing 0.05% (v/v) Tween 20 (PBS-T). Dilutions were prepared in PBS-T containing 0.1% (w/v) BSA. The assay was performed in triplicates. The Stimulation Index (SI) was defined as a ratio of the cytokine concentration from protein challenged samples divided by the cytokine concentration from PBS treated samples.

2.7. Statistical analysis

Differences between treatments were evaluated through a one-way analysis of variance (ANOVA). When the ANOVA produced significant differences ($p < 0.05$), a post-hoc Tukey's multiple comparison test was applied.

3. Results

3.1. In silico immunogenicity prediction and de-immunized protein design

Peptide binding to HLA molecules is the critical first step required for a T cell response. In fact, the strength of peptide binding to MHC molecules is one of the most relevant attributes determining protein immunogenicity [42]. In order to analyze the potential immunogenicity of GMOP-IFN, the complete amino acid sequence was screened using EpiMatrix [43]. This study showed a high content of T cell epitopes in the protein sequence (Fig. 1A). A further analysis using the ClustMer algorithm identified high density "clusters" of putative 9-mer MHC binding peptides. A total of six clusters were defined, spanning the following residues: 20–43, 58–72, 70–89, 121–141, 131–154, 158–179. Five out of six predicted MHC binding clusters overlapped with published T cell epitopes [44].

Then, we considered these results along with our previous experimental data where we identified critical residues for protein activity and immunogenicity [25,44]. Thus, we selected and introduced ten mutations into the GMOP-IFN sequence in different combinations. Modifications were made to alanine (except for one mutation that was made to threonine). All these modifications were introduced to generate GMOP-IFN-VAR1 and the impact on T cell epitope content is illustrated in Fig. 1B.

We previously reported that the following modifications in the hIFN-

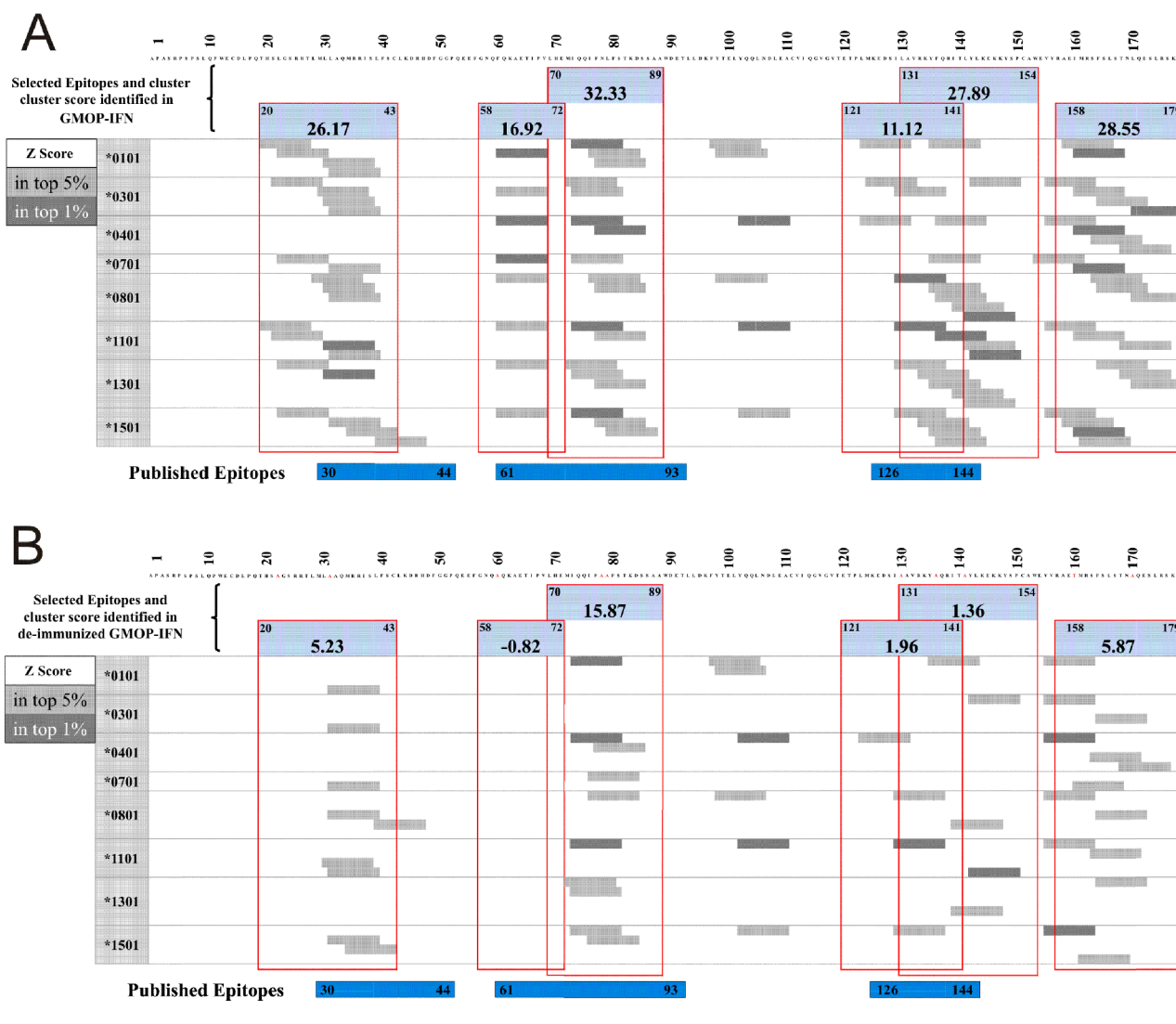


Fig. 1. *In silico* immunogenicity analysis of GMOP-IFN. A) MHC Class II binding cluster as of GMOP-IFN as predicted by EpiMatrix. EpiMatrix-predicted 9-mer hits for 8 prevalent HLA class II alleles are aligned along GMOP-IFN sequence. Peptides scoring above 1.64 on the EpiMatrix “Z” scale (top 5%) are considered to be potential epitopes (gray bars). Peptides scoring above 2.32 on the scale (top 1%) are extremely likely to bind MHC (black bars). Clusters identified by EpiMatrix with the respective scores indicated above are framed in red. Published epitopes (blue bars) determined by experimental methods overlapped with those defined here. B) Impact of selected mutations on the overall potential immunogenicity of GMOP-IFN. (For interpretation of the references to colour in this figure legend, the reader is referred to the web version of this article.)

$\alpha 2b$ molecule: L9A, F47A, L117A, F123A and L128A were critical for binding to specific HLA molecules [25], and therefore were also considered to develop GMOP-IFN-VAR2. We also produced two additional protein variants, GMOP-IFN-VAR3 and GMOP-IFN-VAR4, both carrying seven mutations, in order to reduce the antigenicity of clusters 158–179 and 70–89, respectively (see Table 1). As shown in Fig. 2 the EpiMatrix immunogenicity score [43] for each variant is markedly reduced in comparison with the original molecule.

3.2. GMOP-IFN de-immunized variants: production and purification

GMOP-IFN variants were synthesized and cloned into third-generation lentiviral vectors and then expressed in CHO cells. After cell selection using puromycin ($300 \mu\text{g}\cdot\text{ml}^{-1}$), culture supernatants from stable cell lines were preliminary screened for rhIFN- $\alpha 2b$ production and biological potency by sandwich ELISA and antiviral assays, respectively (data not shown).

For protein purification we performed a one-step immunoaffinity

chromatography using a monoclonal antibody (CA5E6), adsorbed on CNBr-activated Sepharose as ligand. Supernatants-containing protein variants were loaded onto the matrix, without exceeding 40% of its theoretical capacity. No loss of the cytokine was observed either in flowthrough or washing steps. Protein concentration was measured by spectrophotometric absorbance ($\lambda = 280 \text{ nm}$) and purity was analyzed by SDS-PAGE followed by coomassie blue staining (Fig. 3). All GMOP-IFN variants exhibited a main band with a similar mobility compared to non-immunized GMOP-IFN in SDS-PAGE. However, electrophoretic profiles were different, since a band of lower molecular mass was detected in GMOP-IFN-VAR1 and GMOP-IFN-VAR 4 samples; this might correspond to a cleaved glycoform or a contaminant. Contrarily, GMOP-IFN-VAR2 and GMOP-IFN-VAR3 showed a similar molecular mass profile compared to GMOP-IFN. Besides, purity levels of these two variants were also similar to that achieved for GMOP-IFN (over 94%), with the presence of BSA as the main contaminant. In contrast, purity levels of GMOP-IFN-VAR1 and GMOP-IFN-VAR4 were lower, with values about 80%.

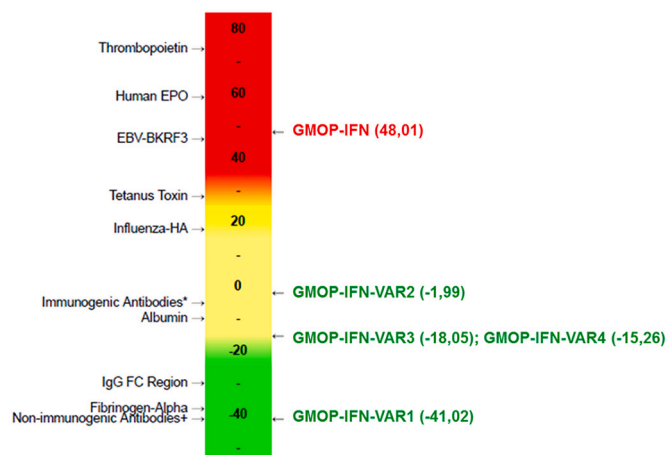


Fig. 2. EpiMatrix MHC binding cluster immunogenicity scale. GMOP-IFN and their deimmunized variants are mapped onto a cluster immunogenicity scale according to their individual EpiMatrix scores. The EpiMatrix cluster immunogenicity score represents the deviation in putative epitope content from baseline expectation based on a random peptide standard. MHC binding clusters scoring above +10 are considered to be potentially immunogenic. Some positive control peptides and proteins are also arranged by EpiMatrix score, from highest (red) to lowest (green). (For interpretation of the references to colour in this figure legend, the reader is referred to the web version of this article.)

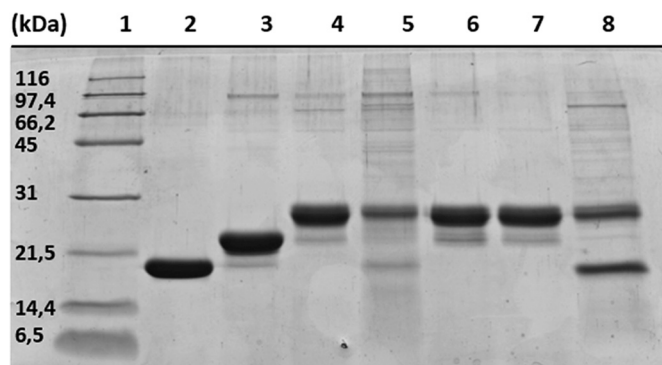


Fig. 3. One-step immunoaffinity chromatography allowed reaching purity levels above 94%. Purity evaluation of different IFN- α analogs by denaturing SDS-PAGE. Lanes: 1- protein molecular weight marker; 2- non-glycosylated IFN; 3- WT-IFN; 4- GMOP-IFN; 5- GMOP-IFN-VAR1; 6- GMOP-IFN-VAR2; 7- GMOP-IFN-VAR3; 8- GMOP-IFN-VAR4.

3.3. GMOP-IFN-VAR2 and GMOP-IFN-VAR3 exhibited high residual antiviral activity and null antiproliferative properties

The deimmunization strategy used in this work was aimed to change the most immunogenic amino acids without altering those residues directly involved in antiviral activity. The impact of those modifications on cytokine's biological activity was evaluated by *in vitro* antiviral activity assays. We used MDBK cells as target for viral infection by VSV virus as this is one of the cell line/virus pairs recommended by the European Pharmacopeia. A marked decrease in residual specific antiviral activity was observed for GMOP-IFN-VAR1 and GMOP-IFN-VAR4 when compared to GMOP-IFN (0.06% and 0.17%, respectively). Consequently, both proteins were discarded from further study. In contrast, as shown in Table 2 GMOP-IFN-VAR2 and GMOP-IFN-VAR3 retained high antiviral activity (72% and 35%, respectively). This suggests that, despite of restricting the selection of immunogenic residues to those not directly involved in biological activity; a partial reduction in the IFN-receptor interaction was still observed.

Table 2

GMOP-IFN-VAR2 and GMOP-IFN-VAR3 retained high residual specific antiviral activity.

GMOP-IFN-VAR1	GMOP-IFN-VAR2	GMOP-IFN-VAR3	GMOP-IFN-VAR4
0.06% \pm 0.02%	72% \pm 4%	35% \pm 2%	0.17% \pm 0.05%

Relative specific antiviral activity with respect to GMOP-IFN (190 \pm 50 IU/ml) was determined by their ability to inhibit the cytopathic effect caused by vesicular stomatitis virus on MDBK cells and normalized to the activity of GMOP-IFN.

During antiviral therapy with rhIFN- α , one of the most common side effects is the decrease in neutrophil counts or neutropenia which is frequently associated with dose adjustment or early discontinuation [45]. To further characterize the antiproliferative activity of GMOP-IFN-VAR2 and GMOP-IFN-VAR3 we used an *in vitro* bioassay to measure their ability to inhibit cell growth of Daudi cells. A marked decrease of the specific antiproliferative activity was observed for both protein variants. As shown in Table 3, both GMOP-IFN-VAR2 and GMOP-IFN-VAR3 exhibited less than 1% of the original antiproliferative potency (reference value for GMOP-IFN is 280 \pm 70 IU- ng^{-1} , while 0.5 \pm 0.2 IU- ng^{-1} and 0.4 \pm 0.1 IU- ng^{-1} were obtained for GMOP-IFN-VAR2 and GMOP-IFN-VAR3, respectively). Taking these results altogether and given that the same cell receptor is involved in both hIFN- α 2b biological activities, this denotes a greater susceptibility of the IFN antiproliferative activity to changes in the amino acid sequence and three dimensional structure.

3.4. GMOP-IFN de-immunized variants showed characteristic electrophoretic profiles

To further characterize the charge-based heterogeneity for each protein variant, we performed an IEF assay. For WT-IFN, rhIFN- α 2b produced in CHO-K1 cells, we observed four electrophoretic bands that represent isoforms with O-glycan structures carrying different content of sialic acid attached to the natural Thr106 O-glycosylation site.

A higher content of glycan structures bound to the potential O-glycosylation sites of GMOP-IFN were evidenced by the presence of approximately 7 isoforms, situated at a more acidic region of the gel. Interestingly, both de-immunized variants showed a different IEF profile when compared with the original molecule. A total of 8 glycoforms were observed for both GMOP-IFN-VAR2 and GMOP-IFN-VAR3, which, as a whole, showed a more acidic profile compared to those of GMOP-IFN, probably indicating a higher content of sialic acid. Moreover, a lower content of the least acidic glycoform of GMOP-IFN-VAR3 (located at the top of the gel) was observed in comparison with the other proteins (Fig. 4). These results are in agreement with the predictions of mucin type GalNAc O-glycosylation sites in mammalian proteins using the NetOGlyc 3.1 server software. This algorithm predicted the occurrence of five O-glycosylation sites for GMOP-IFN and six for GMOP-IFN-VAR2 and GMOP-IFN-VAR3.

3.5. Immunogenicity analysis

Ex vivo human PBMC assays are based on measuring immune cell activation after exposure to therapeutic candidates. The composition of

Table 3

GMOP-IFN-VAR2 and GMOP-IFN-VAR3 exhibited null antiproliferative properties.

Protein	GMOP-IFN-VAR2	GMOP-IFN-VAR3
Specific antiproliferative activity [IU- ng^{-1}]	0.5 \pm 0.04	0.4 \pm 0.1

In vitro specific antiproliferative activity of GMOP-IFN variants measured as their ability to inhibit cell growth of Daudi cells.

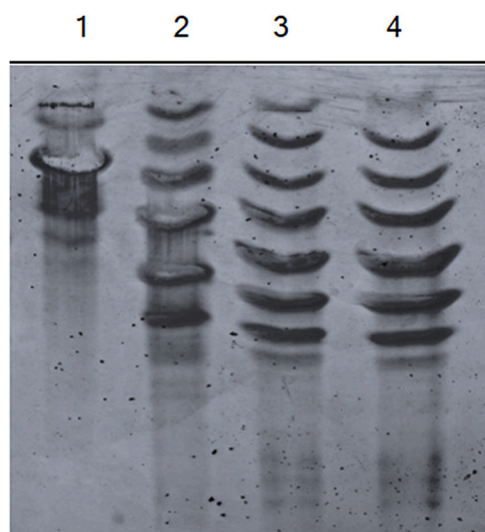


Fig. 4. GMOP-IFN deimmunized variants exhibited a higher content of glycan structures bound to the O-glycosylation moieties. The charge-based heterogeneity of the IFN variants was analyzed by IEF followed by Coomassie blue staining. Differently sialylated forms were distinguished for each protein variant, revealing 7 isoforms for GMOP-IFN and 8 electrophoretic bands for both GMOP-IFN de-immunized variants. Lanes: 1-WT-IFN; 2- GMOP-IFN; 3- GMOP-IFN-VAR2; 4- GMOP-IFN-VAR3.

these samples includes not only some relevant immune cells such as T lymphocytes but also antigen presenting cells (e.g. monocytes, dendritic cells and B cells). Consequently, this constitutes a suitable experimental platform to evaluate the risk associated with the presence of potentially immunogenic T-cell epitopes in therapeutic proteins.

3.5.1. Donor samples

Immune cell-derived assays have been widely used for predicting protein immunogenicity risks [40,46,47]. However, these experiments are more robust when they include heterogeneous HLA genotypes donor pools with good correlation with the HLA occurrence in the world-wide. In particular, in this work we collected blood samples from 26 healthy

Table 4

HLA-DRB1 alleles expressed by donors in our cohort exhibited high heterogeneity.

Donor	Age	Allele	
		DRB1_1	DRB1_2
1	31	DRB1*01	DRB1*04
2	25	DRB1*15	DRB1*15
3	28	DRB1*04	DRB1*13
4	28	DRB1*03	DRB1*04
6	29	DRB1*03	DRB1*08
7	30	DRB1*01	DRB1*03
8	33	DRB1*09	DRB1*11
9	30	DRB1*11	DRB1*16
10	44	DRB1*07	DRB1*13
12	32	DRB1*03	DRB1*08
13	32	DRB1*07	DRB1*11
14	26	DRB1*01	DRB1*13
16	28	DRB1*11	DRB1*15
17	32	DRB1*01	DRB1*16
18	27	DRB1*04	DRB1*15
19	44	DRB1*11	DRB1*15
22	28	DRB1*01	DRB1*03
23	57	DRB1*04	DRB1*13
24	25	DRB1*07	DRB1*11
25	28	DRB1*13	DRB1*16

An aliquot of blood was taken from each donor and HLA-DR allotypes were determined by Luminex Sequencing Technology.

donors. HLA-DRB1 alleles expressed by our cohort exhibited high heterogeneity and are shown in Table 4.

3.5.2. T-cell activation response

The endogenous hIFN- α 2b antiproliferative effect on T-cells restricts its direct incubation with PBMC samples. To circumvent this issue, we adapted an alternative protocol that included a previous step for generation of monocyte-derived DCs (moDCs). Immature DCs were pulsed with the different GMOP-IFN variants during a short incubation time, at a high concentration, and then the cells were washed. During this step immature DCs are able to endocytose and process the antigen. Upon maturation, DCs can present GMOP-IFN-derived peptides bound to MHC class II on the cell surface, where they would be available to stimulate T-cell responses. Blood samples were obtained from healthy donors and selected so as to include most major HLA-DR allotypes expressed in the world population, which enables the detection of any hIFN- α 2b specific T-cell responses restricted to a particular HLA-DR allotype.

As shown in Fig. 5 almost all the donors responded to GMOP-IFN protein, as judged by an increase in IFN- γ production when compared to the negative control. This result is in good agreement with the computational predictions. Also consistent with our findings using the EpiMatrix algorithm, a marked reduction in immunogenicity was observed for both GMOP-IFN de-immunized variants, as evidenced by a reduction of the percentage of IFN- γ responses in 55% of donors for GMOP-IFN-VAR2 and 35% for GMOP-IFN-VAR3. It is important to mention that no IL-4 response was detected in supernatants from cell cultures treated with any GMOP-IFN variant. Nevertheless, it is also important to highlight that IL-4 protein was detectable in cell cultures treated with phytohemagglutinin (data not shown).

3.5.3. HLA-DR restriction for Antigen Presentation

To confirm that antigen presentation was mediated in the context of HLA-DR molecules, GMOP-IFN-pulsed dendritic cells derived from three responsive donors were treated with the anti-HLA-DR monoclonal antibody (clone LN3, mouse IgG2a; Thermo, USA) in two different concentrations before incubation with autologous T-cells. A lower T-cell activation, as judge by a reduction in IFN- γ SI was observed when DCs were previously treated with the anti-DR antibody (Fig. 6). Moreover, this effect was even more pronounced when the added amount of antibody was increased, demonstrating the essential role of HLA-DR molecules for IFN-derived peptide presentation and consequent T-cell activation.

4. Discussion

Emerging viral infections with agents such as SARS-CoV-2, DENV, ZIKV, CHIKV, influenza A, among others, represent a relevant worldwide public health concern. This is due to the rapid spread of their etiologic agents to new areas, the increasing number of human infections and the lack of new therapeutic treatments and/or effective vaccines. To overcome this, several therapeutic strategies are currently in development [48–50]. For instance, the use of rhIFN- α alone or in combination with other synergistic compounds has proven to be effective for the treatment of numerous emerging viral illnesses, such as the infections caused by the recently identified SARS-CoV-2 [1–5]. In addition, several reports have shown favorable synergistic effects of rhIFN- α when combined with clinically-relevant concentrations of favipiravir, sofosbuvir or ribavirin to treat infections with DENV, ZIKV and CHIKV [13,15–17,51].

However, IFN therapy in the clinic is frequently associated with severe side effects such as hematological toxicity, neutropenia and immunogenicity [30,52–55]. Indeed, there is growing evidence showing that repeated dosing over several months induced neutralizing antibodies against the cytokine in a significant number of patients [22,56,57]. The effects of anti-drug antibodies (ADA) vary from binding to the molecule without affecting its efficacy to altering its

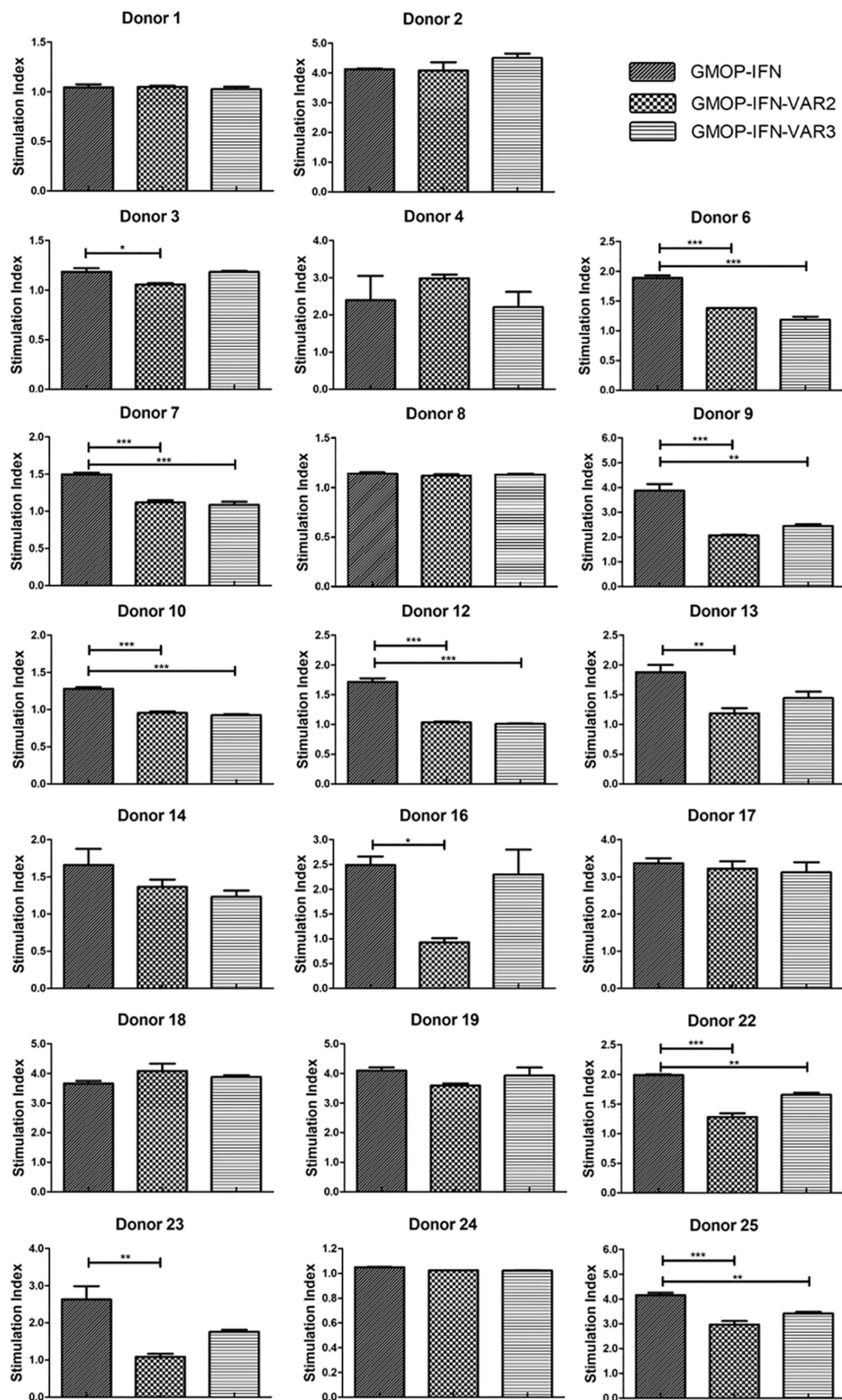


Fig. 5. GMOP-IFN de-immunized variants exhibited a reduced immunogenicity in comparison with the original molecule. Data obtained from 20 donors. IFN- γ secretion by T-cells after incubation with IFN-pulsed dendritic cells was measured by sandwich ELISA. A Stimulation Index (SI) was defined as a ratio of the cytokine concentration from protein challenged samples divided by cytokine concentration from excipient treated samples. Differences between treatments were evaluated through a one-way analysis of variance (ANOVA). Differences were considered statistically significant when $p < 0.05$. A post-hoc Tukey's multiple comparison test was then applied.

pharmacokinetics, neutralizing its activity or even compromising patient safety fostering the development of autoimmune diseases [58–60].

ADAs against therapeutic proteins were detected in a significant number of patients during phase 3 clinical trials of diverse therapeutic candidates leading to treatment interruption [61]. This is the case of

Vatreptacog alfa, a bioengineered rFVII α analog with increased enzymatic activity. Through a group of tools for immunogenicity prediction Lamberth et al. [47] detected the presence of HLA class II neoepitopes in the FVII α analog. These predictions were in good agreement with *ex vivo* stimulation assays data and clinical outcomes, reflecting that high

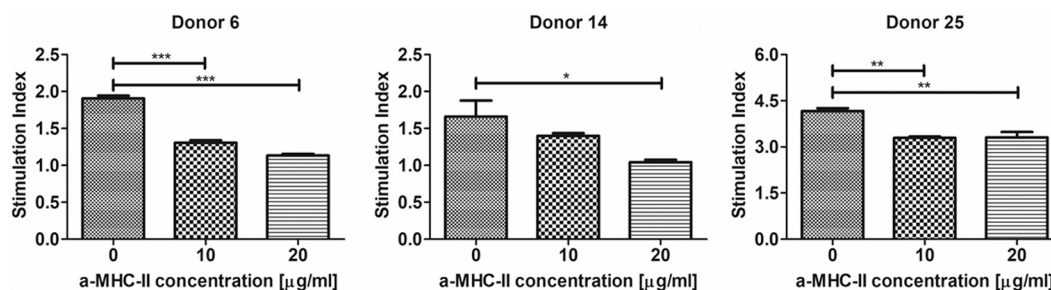


Fig. 6. IFN-derived peptides are presented in the context of HLA-DR molecules. HLA-DR antibody blocking assay to study the HLA restriction of IFN-derived peptide presentation by DC. A successive decrease in IFN- γ SI was observed when two different blocking Ab concentrations were evaluated (a-MHCII 10 μ g/ml or a-MHCII 20 μ g/ml). SI were normalized to the untreated control (excipients).

affinity peptide-MHC binding can effectively lead to epitope recognition and elicitation of a T-cell dependent response that ultimately ends in ADA formation. The notion of kinetic stability of MHCII:peptide complexes as the primary parameter dictating immunodominance has been previously established [42].

In particular, to overcome rhIFN- α immunogenicity risk, we recently carried out a step-wise approach strategy to reduce the number of T-cell epitopes in a hyperglycosylated rhIFN- α 2b version, 4 N-IFN [25]. Two 4N-IFN variants were generated with significant reduced immunogenicity, as determined by *ex vivo* T-cell proliferation assays and cytokine profiling. However, both de-immunized proteins exhibited a marked reduction in their *in vitro* antiviral function. Clinically, this constitutes a limitation due to the large amount of protein to be administered to reach the therapeutic window.

To circumvent this issue, we then designed a new long lasting IFN- α version, referred to as GMOP-IFN. GMOP-IFN is a hIFN- α 2b analog with improved plasma stability and pharmacodynamics properties when compared with the commercial non-glycosylated version [27]. These improved characteristics were reached by adding potential O-glycosylation sites through fusion of a 14-mer peptide to the N-terminus of the protein. Interestingly, this new variant also retained full antiviral activity compared to the unmodified protein, and therefore would constitute an attractive therapeutic candidate in human antiviral therapy.

However, according to *in silico* predictions GMOP-IFN was potentially immunogenic. To address this concern, we used the step-wise strategy to identify immunodominant T-cell epitopes in the sequence and to select the most suitable substitutions to disrupt the HLA:peptide interaction. In order to preserve the cytokine biological function, all mutations were preferentially selected trying to reduce a potential impact on protein structure and receptor binding. Then, using the Epi-Matrix and ClustMer algorithms, predicted MHC-II-binding peptides were grouped into six epitope “clusters” and mapped onto the GMOP-IFN sequence. Five of the identified clusters overlapped with previously identified IFN- α 2b defined epitopes. In order to modify amino acids that contributed the most to MHC Class II binding, we subsequently applied the OptiMatrix tool. Selected MHC binding anchors were replaced with alanine (except for one changed to threonine) to reduce possible negative impact on protein structure and/or biological activity [46]. On the basis of computational prediction results and previous experimental data about critical residues for hIFN- α structure and/or biological function, we designed four variants that were produced in CHO cells. Among them, GMOP-IFN-VAR1 and GMOP-IFN-VAR4, were non-functional and consequently not included for further characterization. Evidently, the mutations introduced in these molecules lead to a disruption in the interaction between IFN and its receptor on MDBK cells. Another reason could be that these modifications increased the site accessibility for O-glycosylation and as a result the glycan structure disrupted the interaction with the IFN receptor on cell surface.

In contrast, the de-immunized variants GMOP-IFN-VAR2 and GMOP-IFN-VAR3 not only retained a significant residual antiviral activity but also exhibited a higher content of highly O-glycosylated isoforms. This supports the notion that an augmented efficiency of GalNAc-transferases attaching the initiating GalNAc monosaccharides to Ser and Thr (and likely some Tyr) residues may be a consequence of the modification of their flanking aminoacids [62]. Also, these results suggest that a lower antiviral activity for IFN analogs might be due to high glycan attachment, which results in both steric hindrances affecting the cytokine-receptor interaction and enhanced repulsive forces with the negatively charged receptor, due to the increased sialic acid content of the protein [63]. This reduction in receptor binding affinity also affected the growth-inhibitory activity but in a markedly higher extent than for antiviral activity. This is in correlation with a previous report showing how IFNs can exert diverse biological or immunological functions through different IFN-receptor interaction stabilities [64,65]. Moreover, it has been assumed that a highly stable IFN-receptor complex is required for triggering the antiproliferative pathway, whereas this would not be so crucial for eliciting an antiviral response [66,67].

Hematologic disorders are a common side effect associated with interferon alpha therapy, characterized by bone marrow suppression and a reduction in white blood cell counts [30]. In particular, high rates of hematological adverse events such as anemia, leukopenia, neutropenia, and thrombocytopenia have been extensively reported in chronic Hepatitis C patients after IFN administration [68]. In fact, therapeutic doses of interferon may decrease neutrophil count by 30%–50%, while causing a dramatic increase in risk of bacterial infections and sepsis [69]. In this context, GMOP-IFN de-immunized variants developed in this study lack antiproliferative properties while preserving antiviral activity, representing interesting therapeutic alternatives for chronic Hepatitis C treatment.

Although a preclinical immunogenicity assessment may not fully correlate with data from clinical trials, is still a very valuable tool. Indeed, a recent study demonstrated a good agreement between the results obtained from this experimental platform and clinical outcomes [47]. Preclinical immunogenicity assessments could also be used to evaluate the potential immunogenicity risk of mutations introduced into a protein sequence to improve drug efficacy.

Through an *ex vivo* procedure that allows estimating the immune response mediated by T-cells, we have evaluated the effect of mutations introduced in each GMOP-IFN variant on the reduction of T-cell epitope content. The results from *ex vivo* T-cell assays suggest a reduced immunogenicity risk for GMOP-IFN-VAR2 and GOMP-IFN-VAR3, when compared with the original molecule. GMOP-IFN-VAR2 was significantly less immunogenic than GMOP-IFN in terms of T-cell activation, as judged by IFN- γ secretion in cell culture supernatants. GMOP-IFN-VAR3 also showed improvements in its immunogenicity properties but to a lesser extent than GMOP-IFN-VAR2.

Protein glycosylation constitutes a suitable strategy that helps improve the stability, pharmacokinetic properties and protein

immunogenicity [70]. However, glycan attachment to therapeutic proteins can also result in unwanted immunogenicity events with diverse consequences [71]. For instance, CHO cells produce immunogenic glycan structures such as N-glycolylneuraminic acid (Neu5Gc) and α -Gal, which constitutes a major safety concern when using this cell line for therapeutic protein production [72–74]. For this reason, future studies will be addressed in order to characterize these entities in GMOP-IFN variants.

Protein stability is a desired property during development of new therapeutic protein candidates. However, an extended half-life in circulation can also be associated with an increased likelihood of protein detection by tissue resident immune components such as dendritic cells, macrophages and b-cells. As a result, protein glycosylation may indirectly impact on protein immunogenicity. On this regards, the use of an animal model capable of mimicking the human immune response, such as tolerance mice or HLA-DR transgenic mice, constitute a suitable alternative to address this issue.

5. Conclusion

In this study we used a step-wise “DeFT” approach to reduce the immunogenicity of a hyperglycosylated hIFN- α 2b variant. In this way, two deimmunized GMOP-IFN variants with high antiviral activity but null antiproliferative action (one of the negative side effects frequently associated with rhIFN- α antiviral therapy) were developed. In addition, these variants exhibited reduced immunogenicity in *in vitro* T-cell assays and cytokine profile characterization. Taking into account the impact of neutropenia and immunogenicity on the effectiveness and safety of hIFN- α therapy in the clinic, the GMOP-IFN variants developed here constitute potential candidates for antiviral treatment of chronic and emerging viral diseases. Nevertheless, further *in vivo* studies using relevant experimental platforms such as HLA-DR transgenic mice, should also be addressed as complementary pre-clinical studies.

Funding

This work was supported by a grant from the Agencia Nacional de Promoción Científica y Tecnológica [PICT-2014-2343], Universidad Nacional del Litoral and Zelltek S.A. ME, NC, MO and EFM are members of Consejo Nacional de Investigaciones Científicas y Técnicas (CONICET, Argentina).

Declaration of Competing Interest

Two of the contributing authors, Anne S. De Groot and William D. Martin, are senior officers and majority shareholders at EpiVax, Inc., a privately owned biotechnology company located in Providence, RI. These authors acknowledge that there is a potential conflict of interest related to their relationship with EpiVax and attest that the work contained in this research report is free of any bias that might be associated with the commercial goals of the company.

Appendix A. Supplementary data

Supplementary data to this article can be found online at <https://doi.org/10.1016/j.clim.2021.108888>.

References

- R. Pereda, D. González, H.B. Rivero, J.C. Rivero, A. Pérez, L.D.R. Lopez, N. Mezquia, R. Venegas, J.R. Betancourt, R.E. Domínguez, R.E. Domínguez, Therapeutic effectiveness of interferon alpha 2b treatment for COVID-19 patient recovery, *J. Interf. Cytokine Res.* 40 (2020) 578, <https://doi.org/10.1089/jir.2020.0188>.
- G. Li, E. De Clercq, Therapeutic options for the 2019 novel coronavirus (2019-nCoV), *Nat. Rev. Drug Discov.* 19 (2020) 149, <https://doi.org/10.1038/d41573-020-00016-0>.
- A. Pandit, N. Bhalani, B.L.S. Bhushan, P. Koradia, S. Gargiya, V. Bhomia, K. Kansagra, Efficacy and safety of pegylated interferon alfa-2b in moderate COVID-19: A phase II, randomized, controlled, open-label study, *Int. J. Infect. Dis.* 105 (2021) 516–521, <https://doi.org/10.1016/j.ijid.2021.03.015>.
- B. Wang, D. Li, T. Liu, H. Wang, F. Luo, Y. Liu, Subcutaneous injection of IFN alpha-2b for COVID-19: an observational study, *BMC Infect. Dis.* 20 (2020) 1–6, <https://doi.org/10.1186/s12879-020-05425-5>.
- Q. Zhou, V. Chen, C.P. Shannon, X.S. Wei, X. Xiang, X. Wang, Z.H. Wang, S. J. Tebbutt, T.R. Kollmann, E.N. Fish, Interferon- α 2b treatment for COVID-19, *Front. Immunol.* 11 (2020) 1–6, <https://doi.org/10.3389/fimmu.2020.01061>.
- B.M. Bakadia, F. He, T. Souho, L. Lamboni, M.W. Ullah, B.O. Boni, A.A.Q. Ahmed, B.M. Mukole, G. Yang, Prevention and treatment of COVID-19: focus on interferons, chloroquine/hydroxychloroquine, azithromycin, and vaccine, *Biomed. Pharmacother.* 133 (2021), 111008, <https://doi.org/10.1016/j.biopha.2020.111008>.
- A. Srikiatkachorn, A. Mathew, A.L. Rothman, Immune-mediated cytokine storm and its role in severe dengue, *Semin. Immunopathol.* 39 (2017) 563, <https://doi.org/10.1007/s00281-017-0625-1>.
- S. Bhatt, P.W. Gething, O.J. Brady, J.P. Messina, A.W. Farlow, C.L. Moyes, J. M. Drake, J.S. Brownstein, A.G. Hoen, O. Sankoh, M.F. Myers, D.B. George, T. Jaenisch, G.R.W. Wint, C.P. Simmons, T.W. Scott, J.J. Farrar, S.I. Hay, The global distribution and burden of dengue, *Nature.* 496 (2013) 504, <https://doi.org/10.1038/nature12060>.
- M.L. Nunes, C.R. Carlini, D. Marinowic, F.K. Neto, H.H. Fiori, M.C. Scotta, P. L.A. Zanella, R.B. Soder, J.C. Da Costa, Microcephaly and Zika virus: A clinical and epidemiological analysis of the current outbreak in Brazil, *J. Pediatr.* 92 (2016) 230, <https://doi.org/10.1016/j.jpeds.2016.02.009>.
- M. Aubry, V.M. Cao-Lormeau, History of arthropod-borne virus infections in French Polynesia, *New Microbes New Infect.* 29 (2019), 100513, <https://doi.org/10.1016/j.nmni.2019.01.009>.
- F. Simon, E. Javelle, M. Oliver, I. Leparç-Goffart, C. Marimoutou, Chikungunya virus infection, *Curr. Infect. Dis. Rep.* 13 (2011) 218, <https://doi.org/10.1007/s11908-011-0180-1>.
- A.M. Powers, Vaccine and therapeutic options to control chikungunya virus, *Clin. Microbiol.* 31 (2017) e00104–e00116, <https://doi.org/10.1128/CMR.00104-16>.
- B. Snyder, S. Goebel, F. Koide, R. Ptak, R. Kalkeri, Synergistic antiviral activity of Sofosbuvir and type-I interferons (α and β) against Zika virus, *J. Med. Virol.* 90 (2018) 8, <https://doi.org/10.1002/jmv.24932>.
- K. Gowin, T. Jain, H. Kosiorek, R. Tibes, J. Camoriano, J. Palmer J, R. Mesa, Pegylated interferon alpha – 2a is clinically effective and tolerable in myeloproliferative neoplasm patients treated off clinical trial, *Leuk. Res.* 54 (2017) 73, <https://doi.org/10.1016/j.leukres.2017.01.006>.
- C.P. Pires De Mello, G.L. Drusano, J.L. Rodriguez, A. Kaushik, A.N. Brown, Antiviral effects of clinically-relevant interferon- α and ribavirin regimens against dengue virus in the Hollow Fiber Infection Model (HFIM), *Viruses.* 10 (2018) 317, <https://doi.org/10.3390/v10060317>.
- S. Briolant, D. Garin, N. Scaramozzino, A. Jouan, J.M. Crance, In vitro inhibition of Chikungunya and Semliki Forest viruses replication by antiviral compounds: synergistic effect of interferon- α and ribavirin combination, *Antivir. Res.* 61 (2004) 111, <https://doi.org/10.1016/j.antiviral.2003.09.005>.
- K.M. Gallegos, G.L. Drusano, D.Z. D’argenio, A.N. Brown, Chikungunya virus: In vitro response to combination therapy with ribavirin and interferon Alfa 2a, *J. Infect. Dis.* 214 (2016) 1192, <https://doi.org/10.1093/infdis/jiw358>.
- N.A. El-Baky, E.M. Redwan, Therapeutic alpha-interferons protein: structure, production, and biosimilar, *Prep. Biochem. Biotechnol.* 45 (2015) 109, <https://doi.org/10.1080/10826068.2014.907175>.
- E.C. Borden, G.C. Sen, G. Uze, R.H. Silverman, R.M. Ransohoff, G.R. Foster, G. R. Stark, Interferons at age 50: past, current and future impact on biomedicine, *Nat. Rev. Drug Discov.* 6 (2007) 975, <https://doi.org/10.1038/nrd2422>.
- J. Bekisz, H. Schmeisser, J. Hernandez, N.D. Goldman, K.C. Zoon, Human interferons alpha, beta and omega, *Growth Factors* 22 (2004) 243, <https://doi.org/10.1080/08977190400000833>.
- D. Al-Zahrani, A. Raddadi, M. Massaad, S. Keles, H.H. Jabara, T.A. Chatila, R. Geha, Successful interferon-alpha 2b therapy for unremitting warts in a patient with DOCK8 deficiency, *Clin. Immunol.* 153 (2014) 104, <https://doi.org/10.1016/j.clim.2014.04.005>.
- C. Scagnolari, S. Trombetti, A. Soldà, M. Milella, G.B. Gaeta, G. Angarano, G. Scotto, N. Caporaso, F. Morisco, R. Cozzolongo, G. Giannelli, M. Fasano, T. Santantonio, G. Antonelli, Development and specificities of anti-interferon neutralizing antibodies in patients with chronic hepatitis C treated with pegylated interferon- α , *Clin. Microbiol. Infect.* 18 (2012) 1033, <https://doi.org/10.1111/j.1469-0691.2011.03729.x>.
- T. Santantonio, M. Milella, G. Antonelli, C. Scagnolari, Neutralizing antibodies to interferon alpha in a chronic hepatitis C patient non-responder to pegylated interferon, *J. Hepatol.* 45 (2006) 759, <https://doi.org/10.1016/j.jhep.2006.08.007>.
- A.A. van der Eijk, J.M. Vrolijk, B.L. Haagmans, Antibodies neutralizing peginterferon alfa during retreatment of hepatitis C, *N. Engl. J. Med.* 354 (2006) 1323, <https://doi.org/10.1056/NEJMc052880>.
- E.F. Mufarrije, S. Giorgetti, M. Etcheverrigaray, F. Terry, W. Martin, A. S., De Groot De-immunized and functional therapeutic (DeFT) versions of a long lasting recombinant alpha interferon for antiviral therapy, *Clin. Immunol.* 176 (2017) 31, <https://doi.org/10.1016/j.clim.2017.01.003>.
- N. Ceaglio, M. Etcheverrigaray, R. Kratje, M. Oggero, Novel long-lasting interferon alpha derivatives designed by glycoengineering, *Biochimie.* 90 (2008) 437, <https://doi.org/10.1016/j.biochi.2007.10.013>.

- [27] M. de los Sales, R. Kratje, M. Oggero, N. Ceaglio, Bifunctional GM-CSF-derived peptides as tools for O-glycoengineering and protein tagging, *J. Biotechnol.* 327 (2021) 18, <https://doi.org/10.1016/j.jbiotec.2020.12.016>.
- [28] L. Moise, C. Song, W.D. Martin, R. Tassone, A.S. De Groot, D.W. Scott, Effect of HLA DR epitope de-immunization of factor VIII in vitro and in vivo, *Clin. Immunol.* 142 (2012) 320, <https://doi.org/10.1016/j.clim.2011.11.010>.
- [29] A.S. De Groot, W. Martin, Reducing risk, improving outcomes: bioengineering less immunogenic protein therapeutics, *Clin. Immunol.* 131 (2009) 189, <https://doi.org/10.1016/j.clim.2009.01.009>.
- [30] A. Soza, J.E. Everhart, M.G. Ghany, E. Doo, T. Heller, K. Promrat, Y. Park, T. J. Liang, J.H. Hoofnagle, Neutropenia during combination therapy of interferon alfa and ribavirin for chronic hepatitis C, *Hepatology.* 36 (2002) 1273, <https://doi.org/10.1053/jhep.2002.36502>.
- [32] S. Southwood, J. Sidney, A. Kondo, M.F. del Guercio, E. Appella, S. Hoffman, R. T. Kubo, R.W. Chesnut, H.M. Grey, A. Sette, Several common HLA-DR types share largely overlapping peptide binding repertoires, *J. Immunol.* 160 (1998) 3363.
- [33] A.S. De Groot, Immunomics: discovering new targets for vaccines and therapeutics, *Drug Discov. Today* 11 (2006) 203, [https://doi.org/10.1016/S1359-6446\(05\)03720-7](https://doi.org/10.1016/S1359-6446(05)03720-7).
- [34] L. Naldini, U. Blömer, P. Gally, D. Ory, R. Mulligan, F.H. Gage, I.M. Verma, D. Trono, In vivo gene delivery and stable transduction of nondividing cells by a lentiviral vector, *Science.* (80-) 272 (1996) 263, <https://doi.org/10.1126/science.272.5259.263>.
- [35] T. Dull, R. Zufferey, M. Kelly, R.J. Mandel, M. Nguyen, D. Trono, L. Naldini, A third-generation lentivirus vector with a conditional packaging system, *J. Virol.* 72 (1998) 8463.
- [36] K. Julenius, A. Mølgaard, R. Gupta, S. Brunak, Prediction, conservation analysis, and structural characterization of mammalian mucin-type O-glycosylation sites, *Glycobiology.* 15 (2005) 153, <https://doi.org/10.1093/glycob/cwh151>.
- [37] P.C. Familletti, S. Rubinstein, S. Pestka, A convenient and rapid cytopathic effect inhibition assay for interferon, *Methods Enzymol.* 78 (1981) 387, [https://doi.org/10.1016/0076-6879\(81\)78146-1](https://doi.org/10.1016/0076-6879(81)78146-1).
- [38] S. Rubinstein, P.C. Familletti, S. Pestka, Convenient assay for interferons, *J. Virol.* 37 (1981) 755, <https://doi.org/10.1128/jvi.37.2.755-758.1981>.
- [39] T. Nederman, E. Karlström, L. Sjödin, An in vitro bioassay for quantitation of human interferons by measurements of antiproliferative activity on a continuous human lymphoma cell line, *Biologicals.* 18 (1990) 29, [https://doi.org/10.1016/1045-1056\(90\)90066-9](https://doi.org/10.1016/1045-1056(90)90066-9).
- [40] A. Jaber, M. Baker, Assessment of the immunogenicity of different interferon beta-1a formulations using ex vivo T-cell assays, *J. Pharm. Biomed. Anal.* 43 (2007) 1256, <https://doi.org/10.1016/j.jpba.2006.10.023>.
- [41] E. Elkord, P.E. Williams, H. Kynaston, A.W. Rowbottom, Human monocyte isolation methods influence cytokine production from in vitro generated dendritic cells, *Immunology.* 114 (2005) 204, <https://doi.org/10.1111/j.1365-2567.2004.02076.x>.
- [42] C.A. Lazarski, F.A. Chaves, S.A. Jenks, S. Wu, K.A. Richards, J.M. Weaver, A. J. Sant, The kinetic stability of MHC class II: peptide complexes is a key parameter that dictates immunodominance, *Immunity.* 23 (2005) 29, <https://doi.org/10.1016/j.immuni.2005.05.009>.
- [43] V. Jawa, F. Terry, J. Gokemeijer, S. Mitra-Kaushik, B.J. Roberts, S. Tourdot, A.S. De Groot, T-cell dependent immunogenicity of protein therapeutics pre-clinical assessment and mitigation—updated consensus and review 2020, *Front. Immunol.* 11 (2020) 1301.
- [44] T.D. Jones, M. Hanlon, B.J. Smith, C.T. Heise, P.D. Nayee, D.A. Sanders, A. Hamilton, C. Sweet, E. Unitt, G. Alexander, L. Kin-Ming, S.D. Gillies, F.J. Carr, M.P. Baker, The development of a modified human IFN- α 2b linked to the fc portion of human IgG1 as a novel potential therapeutic for the treatment of hepatitis C virus infection, *J. Interf. Cytokine Res.* 24 (2004) 560, <https://doi.org/10.1089/jir.2004.24.560>.
- [45] M.I. Saleh, N.N. Hindi, A population pharmacodynamic model characterizing neutropenia associated with pegylated interferon alpha 2-a therapy in patients with chronic hepatitis C viral infection, *Naunyn Schmiedeberg's Arch. Pharmacol.* 391 (2018) 953, <https://doi.org/10.1007/s00210-018-1517-1>.
- [46] R. Mazor, A.N. Vassall, J.A. Eberle, R. Beers, J.E. Weldon, D.J. Venzon, K.Y. Tsang, I. Benhar, I. Pastan, Identification and elimination of an immunodominant T-cell epitope in recombinant immunotoxins based on *Pseudomonas exotoxin A*, *Proc. Natl. Acad. Sci. U. S. A.* 109 (2012) 3597, <https://doi.org/10.1073/pnas.1218138109>.
- [47] K. Lamberth, S.L. Reedtz-Runge, J. Simon, K. Klementyeva, G.S. Pandey, S. B. Padkjær, V. Pascal, I.R. León, C.N. Gudme, S. Buus, Z.E. Sauna, Post hoc assessment of the immunogenicity of bioengineered factor VIIa demonstrates the use of preclinical tools, *Sci. Transl. Med.* 9 (2017) eaag1286, <https://doi.org/10.1126/scitranslmed.aag1286>.
- [48] D. Mani, A. Wadhvani, P.T. Krishnamurthy, Drug repurposing in antiviral research: a current scenario, *J. Young. Pharm.* 11 (2019) 117, <https://doi.org/10.5530/jyp.2019.11.26>.
- [49] S.M. Bhat, P.P. Mudgal, N. Sudheesh, G. Arunkumar, Spectrum of candidate molecules against chikungunya virus - an insight into the antiviral screening platforms, *Expert Rev. Anti-Infect. Ther.* 17 (2019) 243, <https://doi.org/10.1080/14787210.2019.1595591>.
- [50] J.M. Shim, J. Kim, T. Tenson, J.Y. Min, D.E. Kainov, Influenza virus infection, interferon response, viral counter-response, and apoptosis, *Viruses.* 9 (2017) 223, <https://doi.org/10.3390/v9080223>.
- [51] C.P. Pires De Mello, X. Tao, T.H. Kim, J.B. Bulitta, J.L. Rodriguez, J.J. Pomeroy, A. N. Brown, Zika virus replication is substantially inhibited by novel favipiravir and interferon alpha combination regimens, *Antimicrob. Agents Chemother.* 62 (2018), <https://doi.org/10.1128/AAC.01983-17> e01983-17.
- [52] M. Wada, H. Marusawa, R. Yamada, A. Nasu, Y. Osaki, M. Kudo, M. Nabeshima, Y. Fukuda, T. Chiba, F. Matsuda, Association of genetic polymorphisms with interferon-induced haematologic adverse effects in chronic hepatitis C patients, *J. Viral Hepat.* 16 (2009) 388, <https://doi.org/10.1111/j.1365-2893.2009.01095.x>.
- [53] Y. Oppenheim, Y. Ban, Y. Tomer, Interferon induced autoimmune thyroid disease (AITD): a model for human autoimmunity, *Autoimmun. Rev.* 3 (2004) 388, <https://doi.org/10.1016/j.autrev.2004.03.003>.
- [54] S. Yilmaz, K. Akar Cimen, Pegylated interferon alfa-2B induced lupus in a patient with chronic hepatitis B virus infection: case report, *Clin. Rheumatol.* 28 (2009) 1241, <https://doi.org/10.1007/s10067-009-1239-3>.
- [55] C. Jorns, D. Holzinger, R. Thimme, H.C. Spangenberg, M. Weidmann, J. Rasenack, H.E. Blum, O. Haller, G. Kochs, Rapid and simple detection of IFN-neutralizing antibodies in chronic hepatitis C non-responsive to IFN- α , *J. Med. Virol.* 78 (2006) 74, <https://doi.org/10.1002/jmv.20506>.
- [56] K.U. Nolte, G. Günther, P. von Wussow, Epitopes recognized by neutralizing therapy-induced human anti-interferon alpha antibodies, *Eur. J. Immunol.* 26 (1996) 2155.
- [57] P. Halfon, S. Pérusat, M. Bourlière, J.P. Bronowicki, P. Trimoulet, Y. Benhamou, V. Leroy, P. Marcellin, J. Foucher, G. Penaranda, G. Chêne, P. Couzigou, Neutralizing antibodies to interferon- α and circulating interferon in patients with chronic hepatitis C non-responding to pegylated interferon plus ribavirin re-treated by pegylated interferon- α 2a and ribavirin (ANRS HCl6 GAMMATRI substudy), *J. Med. Virol.* 82 (2010) 2027, <https://doi.org/10.1002/jmv.21909>.
- [58] A.S. De Groot, D.W. Scott, Immunogenicity of protein therapeutics, *Trends Immunol.* 28 (2007) 482, <https://doi.org/10.1016/j.it.2007.07.011>.
- [59] F. Groell, O. Jordan, G. Borchard, In vitro models for immunogenicity prediction of therapeutic proteins, *Eur. J. Pharm. Biopharm.* 130 (2018) 128, <https://doi.org/10.1016/j.ejpb.2018.06.008>.
- [60] Z.E. Sauna, D. Lagassé, J. Pedras-Vasconcelos, B. Golding, A.S. Rosenberg, Evaluating and mitigating the immunogenicity of therapeutic proteins, *Trends Biotechnol.* 36 (2018) 1068, <https://doi.org/10.1016/j.tibtech.2018.05.008>.
- [61] J.N. Mahlangu, K.N. Weldingh, S.R. Lentz, S. Kaicker, F.A. Karim, T. Matsushita, M. Recht, W. Tomczak, J. Windyga, S. Ehrenforth, K. Knoke, Changes in the amino acid sequence of the recombinant human factor VIIa analog, vatreceptac alfa, are associated with clinical immunogenicity, *J. Thromb. Haemost.* 2015 (1989) 13, <https://doi.org/10.1111/jth.13141>.
- [62] C. Steentoft, S.Y. Vakhrushev, H.J. Joshi, Y. Kong, M.B. Vester-Christensen, K. T. Schjoldager, K. Lavrsen, S. Dabelsteen, N.B. Pedersen, L. Marcos-Silva, R. Gupta, E.P. Bennett, U. Mandel, S. Brunak, H.H. Wandall, S.B. Levery, H. Clausen, Precision mapping of the human O-GalNAc glycoproteome through SimpleCell technology, *EMBO J.* 32 (2013) 1478, <https://doi.org/10.1038/emboj.2013.79>.
- [63] N. Ceaglio, M. Etcheverrigaray, R. Kratje, M. Oggero, Influence of carbohydrates on the stability and structure of a hyperglycosylated human interferon alpha mutein, *Biochimie* 92 (2010) 971, <https://doi.org/10.1016/j.biochi.2010.04.004>.
- [64] C. Thomas, I. Moraga, D. Levin, P.O. Krutzik, Y. Podoplelova, A. Trejo, C. Lee, G. Yarden, S.E. Vleck, J.S. Glenn, G.P. Nolan, J. Piehler, G. Schreiber, K.C. Garcia, Structural linkage between ligand discrimination and receptor activation by type I interferons, *Cell.* 146 (2011) 621, <https://doi.org/10.1016/j.cell.2011.06.048>.
- [65] J. Piehler, C. Thomas, K.C. Garcia, G. Schreiber, Structural and dynamic determinants of type I interferon receptor assembly and their functional interpretation, *Immunol. Rev.* 250 (2012) 317, <https://doi.org/10.1111/imr.12001>.
- [66] J. Ghislain, G. Sussman, S. Goelz, L.E. Ling, E.N. Fish, Configuration of the interferon- α/β receptor complex determines the context of the biological response, *J. Biol. Chem.* 270 (1995) 21785, <https://doi.org/10.1074/jbc.270.37.21785>.
- [67] P. Lamken, S. Lata, M. Gavutis, J. Piehler, Ligand-induced assembling of the type I interferon receptor on supported lipid bilayers, *J. Mol. Biol.* 341 (2004) 303, <https://doi.org/10.1016/j.jmb.2004.05.059>.
- [68] M.F. Montasser, S. Zaky, M. Salaheldin, D. Johar, A.I. Abushouk, F. El-Raey, M. Al-Husseini, E.G. Mohammed, Fib-4 predicts early hematological adverse events induced by interferon-based triple therapy in chronic hepatitis C virus patients, *J. Interf. Cytokine Res.* 39 (2019) 85, <https://doi.org/10.1089/jir.2018.0131>.
- [69] N.N. Hindi, M.I. Saleh, Patient characteristics associated with pegylated interferon alfa-2a induced neutropenia in chronic hepatitis C patients, *Clin. Exp. Pharmacol. Physiol.* 45 (2018) 636, <https://doi.org/10.1111/1440-1681.12934>.
- [70] A. Gugliotta, M.J. Leopold, E. Mufarrije, M. Etcheverrigaray, R. Kratje, N. Ceaglio, M. Oggero, Pharmacokinetics versus in vitro Antiproliferative potency to design a novel Hyperglycosylated hIFN- α 2 biobetter, *Pharm. Res.* 38 (2021) 37–50, <https://doi.org/10.1007/s11095-020-02978-7>.
- [71] M.J. Buettner, S.R. Shah, C.T. Saeui, R. Ariss, K.J. Yarema, Improving immunotherapy through glycodeSIGN, *Front. Immunol.* 9 (2018), <https://doi.org/10.3389/fimmu.2018.02485>.
- [72] D. Ghaderi, M. Zhang, N. Hurtado-Ziola, A. Varki, Production platforms for biotherapeutic glycoproteins. Occurrence, impact, and challenges of non-human sialylation, *Biotechnol. Genet. Eng. Rev.* 28 (2012) 147–175, <https://doi.org/10.5661/bger-28-147>.
- [73] R. Amon, E.M. Reuven, S. Leviatan Ben-Arye, V. Padler-Karavani, Glycans in immune recognition and response, *Carbohydr. Res.* 389 (2014) 115–122, <https://doi.org/10.1016/j.carres.2014.02.004>.
- [74] S. Yehuda, V. Padler-Karavani, Glycosylated biotherapeutics: immunological effects of N-glycolylneuraminic acid, *Front. Immunol.* 11 (2020) 1–9, <https://doi.org/10.3389/fimmu.2020.00021>.